JOURNAL OF PETROLOGY | VOLUME 41 | NUMBER 4 | PAGES 545–561 | 2000

Noble Metal Enrichment Processes in the Merensky Reef, Bushveld Complex

CHRIS BALLHAUS[1,2]* AND PAUL SYLVESTER[1]†

[1]RSES, AUSTRALIAN NATIONAL UNIVERSITY, CANBERRA, A.C.T. 0200, AUSTRALIA

[2]GEOLOGY DEPARTMENT, AUSTRALIAN NATIONAL UNIVERSITY, CANBERRA, A.C.T. 0200, AUSTRALIA

RECEIVED FEBRUARY 8, 1999; REVISED TYPESCRIPT ACCEPTED SEPTEMBER 27, 1999

We have analysed sulphides, silicates, and chromites of the Merensky Reef for platinum-group elements (PGEs), Re and Au using laser ablation-inductively coupled plasma mass spectrometry and synthetic pyrrhotite standards annealed with known quantities of noble metals. Os, Ir and Ru reside in solid solution in pyrrhotite and pentlandite, Rh and part of the Reef's Pd in pentlandite, whereas Pt, Au, Re and some Pd form discrete phases. Olivine and chromite, often suspected to carry Os, Ir and Ru, are PGE free. All phases analysed contain noble metals as discrete micro-inclusions with diameters typically <100 nm. Inclusions in sulphides commonly have the element combinations Os–Ir–Pt and Pt–Pd–Au. Inclusions in olivine and chromite are dominated by Pt ± Au–Pd. Few inclusion spectra can be related to discrete noble metal phases, and few inclusions have formed by sub-solidus exsolution. Rather, some PGE inclusions, notably those in olivine and chromite, are early-magmatic nuggets trapped when their host phases crystallized. We suggest that the silicate melt layer that preceded the Merensky Reef was PGE oversaturated at early cumulus times. Experiments combined with available sulphide–silicate partition coefficients suggest that a silicate melt in equilibrium with a sulphide melt containing the PGE spectrum of the Merensky ore would indeed be oversaturated with respect to the least soluble noble metals. Sulphide melt apparently played little role in enriching the noble metals in the Merensky Reef; rather, its role was to immobilize a pre-existing in situ *stratiform PGE anomaly in the liquid-stratified magma chamber.*

KEY WORDS: *Bushveld Complex; Merensky Reef; laser-ablation ICP-MS; platinum-group mineralization*

*Corresponding author. Present address: Institut für Mineralogie, Universität Münster, Corrensstr. 24, 48149 Münster, Germany. Telephone: +49-0251-8333047. Fax: +49-0251-8338397. e-mail: chrisb@nwz.uni-muenster.de

†Present address: Department of Earth Sciences, Memorial University of Newfoundland, St John's, NF, A1B 3X5, Canada.

INTRODUCTION

The enrichment of noble metals in layered gabbroic intrusions to form stratiform Merensky-type ore horizons is an extremely efficient yet poorly understood process. Metal enrichment must be related to the formation of magmatic layering, as the ore horizons form an integral part of the magmatic stratigraphies of their host intrusions. Metal concentration is also related to the presence of magmatic sulphides, because the noble metals are either dissolved in base metal sulphides or occur as discrete noble mineral phases intergrown with sulphides (Vermaak & Hendriks, 1976; Ballhaus & Ryan, 1995; Ballhaus & Ulmer, 1995).

There is considerable controversy as to where the metals came from and how metal enrichment worked. For a stratiform platinum-group element (PGE) deposit inside the magmatic stratigraphy of a layered intrusion, there are two possibilities: either the metals were derived from the melt column above the ore horizon, or they came from the magma equivalent to the cumulate package underlying the ore. Owing to the large density contrast between silicate and sulphide melt, a popular view is that the metals were enriched by gravitational settling of sulphide melt, i.e. out of the magma column above the ore (Campbell *et al.*, 1983; Barnes & Naldrett, 1985; Naldrett *et al.*, 1987). On the other hand, it is well established that gravitational crystal settling plays little role in producing magmatic layering and magmatic stratigraphies (McBirney & Noyes, 1979; Morse, 1986; Campbell, 1987), and this cannot remain without consequence for stratiform noble metal deposits.

A third alternative is noble metal enrichment by late- to post-magmatic fluids. The Merensky Reef contains high-temperature saline fluid inclusions (Ballhaus &

Stumpfl, 1986), and the J-M Reef in the Stillwater Complex hosts Cl-rich apatite that grew in the presence of an exsolved saline fluid (Boudreau *et al.*, 1986). However, it was not demonstrated that these fluids were also instrumental in concentrating the PGEs. Nor is it obvious how a post-cumulus process such as fluid infiltration could leave a PGE anomaly with such strict and laterally persistent stratigraphic control as the Merensky Reef.

In this paper we report the first laser ablation-inductively coupled plasma mass spectrometry (ICP-MS) analyses of sulphides, cumulus olivines, and chromites of the Merensky Reef in the Bushveld Complex (Rustenburg, South Africa). Originally, the study was initiated to better understand how PGEs partition between sulphides during recrystallization of monosulphide solid solution (mss). In the course of this work we have detected a hitherto unreported suite of polymetallic PGE microinclusions, in sulphides, cumulus olivine, and chromite. Based on these inclusions, we challenge the widely accepted '*R*-factor' model for PGE enrichment of Campbell *et al.* (1983) and Naldrett *et al.* (1987). We substantiate the hypothesis, originally by Tredoux *et al.* (1995), that the Merensky silicate melt was oversaturated with some PGEs before sulphide saturation occurred. Exsolution of the sulphide melt merely immobilized a pre-existing stratiform PGE anomaly in the liquid-stratified magma chamber.

PETROLOGY OF THE MERENSKY REEF AND THE *R*-FACTOR MODEL

The Merensky Reef is a sulphide-bearing, PGE-rich cumulate horizon in the upper critical zone of the Bushveld Complex, South Africa. In its most typical development (Fig. 1a) it consists of a pyroxenitic pegmatoid orthocumulate of 20–25 cm thickness underlain by a chromitite seam of several centimetres thickness. Along the top contact the pegmatoid is often rimmed by another, less persistent chromite stringer. Normally, the chromite–pegmatoid–chromite package, known as normal Merensky Reef, rests on an undulated, chemically and thermally resorbed, anorthosite to norite footwall. It should be noted that other facies types exist, notably around and within footwall disturbances known as potholes (Fig. 1b–d).

Geochemically, the most interesting components of the Reef are the sulphides and associated PGE phases. Although minor (1–3 vol. %) constituents only, the precursor to the sulphides and PGE phases, i.e. a magmatic sulphide liquid, must have been extraordinarily enriched in PGEs if all PGEs were originally dissolved in the melt phase. At present, the sulphides are equilibrated to low-temperature pyrrhotite, pentlandite and chalcopyrite, sometimes oxidized to pyrite and magnetite, and most of the PGEs have exsolved to form discrete mineral phases (see Vermaak & Hendriks, 1976; Ballhaus & Ulmer, 1995).

Recalculating the average ore grades of the Merensky Reef to 100% sulphide gives ~500 ppm combined PGE plus Au in the sulphide fraction, in the proportions summarized in Table 1 (Naldrett *et al.*, 1987). To explain this enrichment, Campbell *et al.* (1983) formulated the '*R*-factor model', which has since been accepted widely as the valid mineralization model for PGE-rich sulphides in layered intrusions (see Naldrett *et al.*, 1987). The model can be stated as follows: a new batch of primitive basaltic melt enters the Bushveld chamber at 'Merensky times' and mixes vigorously with more fractionated resident liquid; as mixing proceeds, finely dispersed droplets of sulphide liquid exsolve, are entrained in the convecting magma, and come into contact with large volumes of silicate melt (high *R*-factor); sulphide scavenges all elements with high sulphide–silicate partition coefficients, notably the PGEs; following a period of cooling, sulphide-laden magma 'downspouts' to sink onto the anorthositic bottom of the magma chamber, coalesces, and then crystallizes to form the laterally continuous Merensky Reef.

The fundamental problem with the *R*-factor model is that it cannot explain both the absolute PGE enrichment and the relative PGE abundances in the sulphide concentrate (Table 1). This is best demonstrated by looking at the equation relating the concentration of a given PGE in the sulphide melt to the concentration of PGEs in the silicate melt, the sulphide–silicate partition coefficient (D), and the silicate–sulphide mass ratio (R):

$$\mathrm{conc}^{\mathrm{PGE}}{}_{\mathrm{sulphide}} = \mathrm{conc}^{\mathrm{PGE}}{}_{\mathrm{silicate}} \times D \times (R + 1)/(R + D).$$

For small R-factors the terms D and $(R + D)$ nearly cancel and the concentration of a given PGE in the sulphide melt is dominated by R. For very large R-factors, the terms $(R + 1)$ and $(R + D)$ will cancel and the concentration of the PGE is a function of the partition coefficient. Thus, the smaller the amount of sulphide relative to the silicate melt, the more the PGE abundance pattern in the sulphide will be dominated by differences in the PGE sulphide–silicate partition coefficients.

Figure 2a compares the PGE spectrum of the magnesian basaltic suite (Davies & Tredoux, 1985), inferred to be a silicate parent melt to the Merensky Reef, with the PGE spectrum of the sulphide concentrate (Table 1). It is obvious that the PGE pattern in the concentrate is practically identical to the pattern in the silicate parent, perhaps apart from a slight positive Pt anomaly and a minor deficit in Au. The graphs in Fig. 2b–d show calculated relative and absolute PGE abundances for three silicate–sulphide mass ratios (*R*-factors) using a set of partition coefficients compiled from the literature by Ballhaus & Ryan (1995). Only with an *R*-factor of

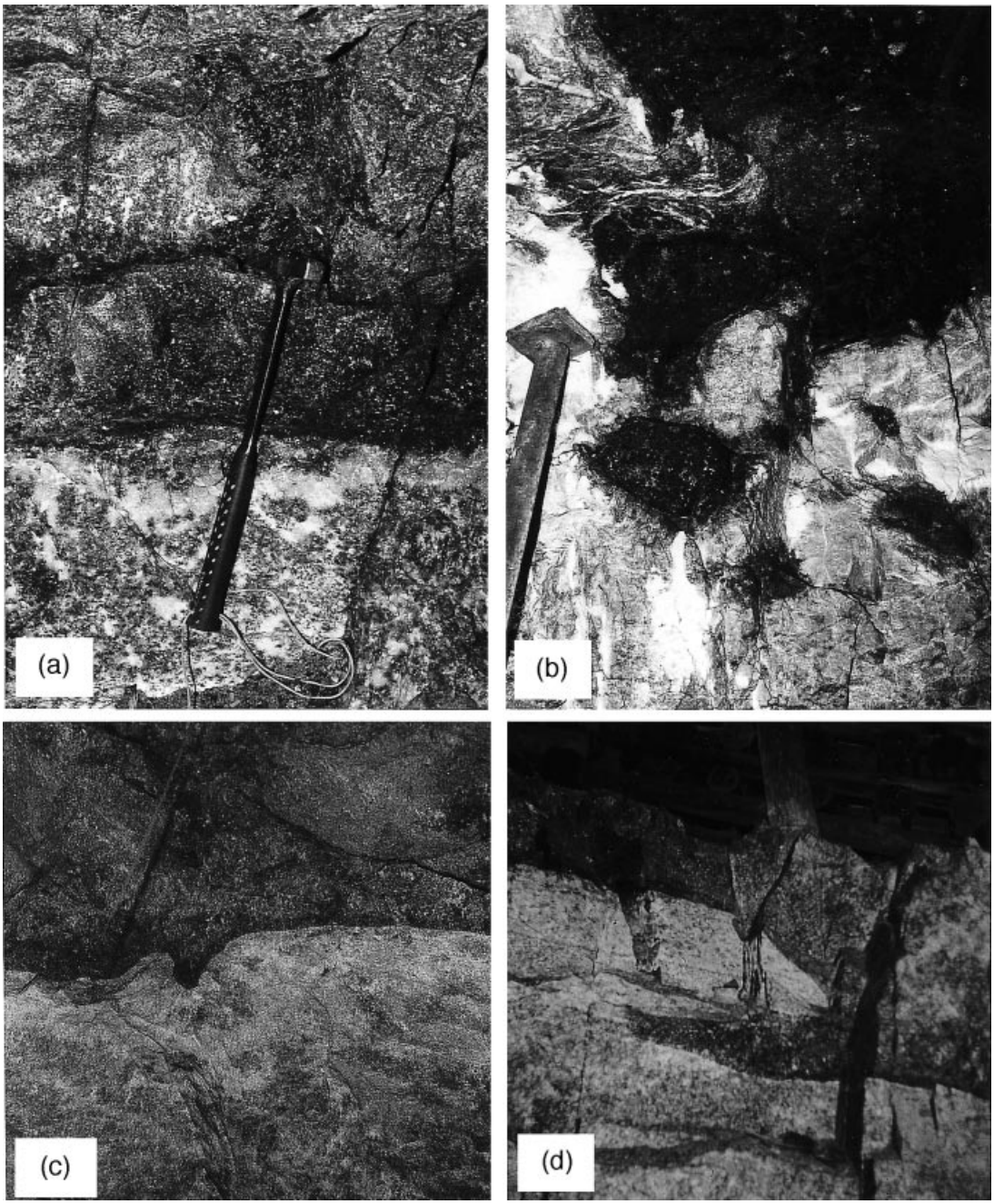

Fig. 1. Typical Merensky Reef facies at Brakspruit shaft, western Bushveld Complex near Rustenburg. (a) The normal pegmatoidal Reef with well-developed bottom and top chromitite seams resting on a resorbed anorthosite footwall. (b) Deep harzburgite pegmatoid Reef in a pothole intersecting the Boulder Bed ~22 m below normal stratigraphic elevation. (c) Rolling contact Reef (chromite only) near a pothole disturbance, sometimes also along overturned pothole flanks. (d) Sulphide-rich pegmatoidal pothole Reef undercutting the footwall marker at a pothole flank. Undercuts like this can be mineralized for several metres (Ballhaus, 1988).

~100 000 (Campbell *et al.*, 1983) does the sulphide reach the PGE concentration of the ore; however, with such a large *R*-factor the PGE pattern now reflects differences in *D* and bears little resemblance to the pattern of the natural sulphide concentrate in Fig. 2a.

In Fig. 3 we repeat the calculation for $R = 100\,000$ with four more sets of experimental *D* values (Bezmen *et al.*, 1994; Fleet *et al.*, 1996; Crocket *et al.*, 1997). Out of these, the *D* values of Fleet *et al.* (1996) give the best match. However, considering the strong dependence of

Table 1: PGE concentrations of the sulphide concentrate of the Merensky Reef, in ppm (after Naldrett et al.*, 1987)*

Os	Ir	Ru	Rh	Pt	Pd	Au
5·2	7·8	35	19	279	120	22

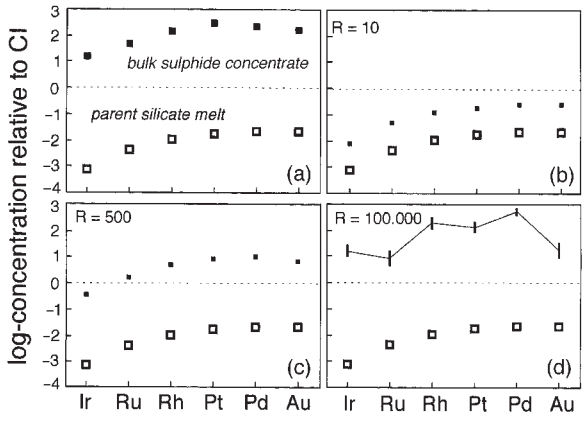

Fig. 2. Calculated and observed PGE patterns [relative to CI from Anders & Grevesse (1989)]. (a) The PGE spectrum of the sulphide concentrate of the Merensky Reef (Naldrett *et al.*, 1987) compared with the PGE spectrum of the high Mg-basaltic suite of Davies & Tredoux (1985). (b–d) Calculated PGE patterns in sulphide melt in equilibrium with Davies & Tredoux's (1985) melt for three *R*-factors and a selection of partition coefficients compiled by Ballhaus & Ryan (1995).

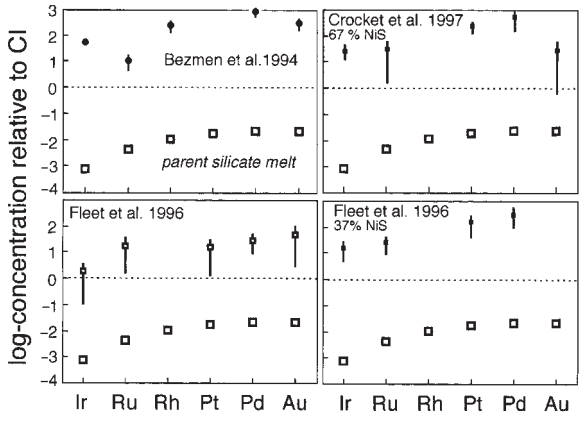

Fig. 3. Calculated PGE abundances in sulphide melt with four internally consistent sets of sulphide–silicate partition coefficients for $R = 100\,000$.

the *D* values of Fleet *et al.* (1996) and Crocket *et al.* (1997) on absolute PGE concentrations in their charges (see below), this agreement may reflect the possibility that some of their charges were PGE oversaturated.

We feel that the PGE pattern of the sulphide concentrate cannot be explained by simple sulphide–silicate equilibration. Unless the sulphide–silicate partition coefficients for all PGEs are the same, which we consider rather unlikely, the *R*-factor model is unable to both explain the PGE enrichment factors and transpose the original magmatic PGE signature from the silicate into the sulphide melt.

EXPERIMENTAL AND ANALYTICAL DETAILS

Any model that aims to explain PGE enrichment processes needs information as to how the noble metals distribute among the phases. For this purpose, we have analysed sulphides, silicates and oxides of the Merensky Reef using laser ablation-ICP-MS (Perkins & Pearce, 1995). The laser microprobe has much lower detection limits than the proton probe. In addition, it discriminates between PGEs in solid solution and PGEs in micro-inclusions. The samples analysed are polished Merensky Reef sulphides from Brakspruit shaft, western Bushveld Complex, some of which were previously analysed by Ballhaus & Ryan (1995) using proton-induced X-ray emission (PIXE). Sample locations and mineralogical and major element compositions have been given by Ballhaus & Ryan (1995).

Synthesis of standards

Microprobe analysis at trace concentration levels requires reliable standards. Ideally, matrices and PGE concentrations in the standards should be as close as possible to the unknowns, to avoid the necessity of matrix corrections. For the present analyses, we have synthesized our own noble metal standards. The matrix was stoichiometric 1C-pyrrhotite (Merck). This was doped with 3–4 mol % S_x to ensure that the final sulphide at synthesis conditions was slightly metal deficient. Ballhaus & Ulmer (1995) showed that Pt and Pd are orders of magnitude more soluble in oxidized, metal-deficient $Fe_{1-x}S$ than in reduced stoichiometric FeS because PGE substitution in mss requires a certain concentration and a statistical distribution of vacancies in the Fe-sublattice. This principle is also valid for other PGEs (Li *et al.*, 1996). Therefore, extra S was added to avoid PGE exsolution during quenching from high temperature.

The initial FeS–S mixture was homogenized under acetone in an agate mortar to complete dryness. The mix was then divided in eight aliquots (for six PGEs, Re and Au). To each aliquot was added, by microsyringe, a single noble metal as chloride complex. Each standard mixture was then homogenized a second time under

Table 2: Sulphide standard compositions, in ppm

Os	Ir	Ru	Rh	Pt	Pd	Au	Re
6·1	3·6	7·7	8·8	4·7	5·5	11·5	6·2

acetone for about 20 min until complete dryness. The final standard powders were dried overnight to evaporate any remaining moisture.

Standard powders were placed in a 4 mm o.d. SiO_2 glass tube, welded shut, and then annealed in a piston cylinder press at 950°C and 1 GPa for 2 days to homogeneous single-phase PGE-bearing $Fe_{1-x}S$ crystal aggregates (courtesy David Ellis, ANU). As the standards must have theoretical density, runs were cooled isobarically with controlled quenching rates at around 500°C per min to avoid contraction cracks.

All synthesis runs gave homogeneous, polycrystalline PGE-bearing $Fe_{1-x}S$ aggregates nearly free of contraction cracks. About one-half of each run product was analysed by isotope dilution solution ICP-MS to determine actual PGE concentrations. The other half was polished, then checked with the laser microprobe for homogeneity. Standard compositions are reported in Table 2. Measured noble metal concentrations were within 20% of the nominal PGE concentrations added as chloride solution.

The laser ICP-MS microprobe

The ANU laser ablation-ICP-MS system consists of a Lambda Physik LPX 120I pulsed ArF excimer laser coupled to a Fisons VG PlasmaQuad PQ2plus ICP-MS instrument. The instrument, and its use for analysis of noble metal concentrations, has been described by Sylvester & Eggins (1997). The sulphide analyses reported here used a 70 μm diameter spot and a laser repetition rate of 10 Hz. Twenty-two isotopes were measured in peak-hopping mode using one point-per-peak: ^{34}S, ^{59}Co, ^{60}Ni, ^{65}Cu, ^{99}Ru, ^{101}Ru, ^{103}Rh, ^{105}Pd, ^{106}Pd, ^{108}Pd, ^{126}Te, ^{185}Re, ^{187}Re, ^{188}Os, ^{189}Os, ^{191}Ir, ^{193}Ir, ^{194}Pt, ^{195}Pt, ^{197}Au, ^{205}Tl, ^{209}Bi. ^{34}S was used as an internal standard to determine concentrations of Ru, Rh, Pd, Re, Os, Ir, Pt and Au by external calibration against our synthetic sulphide standards.

For quantification of the poly-isotopic PGEs, ^{99}Ru was used rather than ^{101}Ru (possible $^{40}Ar^{61}Ni$ interference); ^{106}Pd rather than ^{105}Pd (possible $^{40}Ar^{65}Cu$ interference) or ^{108}Pd (possible $^{92}Mo^{16}O$ interference); ^{187}Re rather than ^{185}Re (smaller abundance isotope); ^{189}Os rather than ^{188}Os (smaller abundance isotope); ^{193}Ir rather than ^{191}Ir (smaller abundance isotope); and ^{195}Pt rather than ^{194}Pt (smaller abundance isotope). Isotopes of Co, Ni, Cu, Te, Tl and Bi were monitored to determine the presence of elements.

Correction procedures

Each analytical session of unknowns commenced and ended with two to three analyses of each PGE standard, with the unknowns as a single block sandwiched between. A typical quantitative laser analysis takes 60 s preceded by 60 s measurement on gas background. Each analysis leaves a crater on the sulphide around 75 μm deep, translating into an average ablation rate on sulphides of 1·25 μm/s.

To convert count rates into concentrations, we subtracted gas background from each of the isotopes of interest. We also applied two other types of corrections, shown in Fig. 4. Each analysis suffered a drop in count rate by up to 60% over the 60 s ablation time (Fig. 4). This can be explained relatively easily: as the laser ablation pit deepens, less material escapes from the hole to be taken up by the Ar stream and ultimately ionized in the plasma source. To correct for this phenomenon we have extrapolated the spectra back to a reference time, i.e. the start of ablation, e.g. to 70 s in Fig. 4a, to determine the count rate for quantification (cf. Sylvester & Ghaderi, 1997). In addition we made a correction for decreases in instrument sensitivity with time, typically around 30% over 4 h (Fig. 4b). This was done by linear interpolation between the count rates of isotopes in the standards, according to the position in the analytical sequence in which the unknown was measured. We estimate that errors are of the order of 10% relative. Detection limits for the PGEs are some tens of ppb for a 70 μm spot and 10 Hz.

COMPOSITION OF MERENSKY SULPHIDES

Typical sulphide spectra are shown in Fig. 5. Instead of quoting individual analyses for each sample, we summarize the noble metal concentrations averaged for each sample (Tables 3 and 4). Individual concentrations and inter-element relationships are shown in Figs 6 and 7. Of all sulphides of the Merensky Reef, we have only analysed systematically the major phases, i.e. pyrrhotite ($Fe_{1-x}S$), pentlandite [$(Ni,Fe)_9S_8$], chalcopyrite ($CuFeS_2$) and pyrite (FeS_2) [for major element compositions, see Ballhaus & Ryan (1995)]. Out of these, only pyrrhotite and pentlandite carry detectable PGEs in solid solution. Chalcopyrite is comparatively PGE-poor, with abundances at the sub-ppm level. Apparent high abundances of Pd and Rh in Fig. 5 are due to interferences by $^{40}Ar^{65}Cu$ and $^{40}Ar^{63}Cu$, respectively, on ^{105}Pd and ^{103}Rh. Pyrite may contain some inherited PGEs if it formed by *in situ* oxidation of pyrrhotite, but concentrations are low and rather erratic.

The following elemental preferences are observed (see Tables 3 and 4, and Figs 6 and 7):

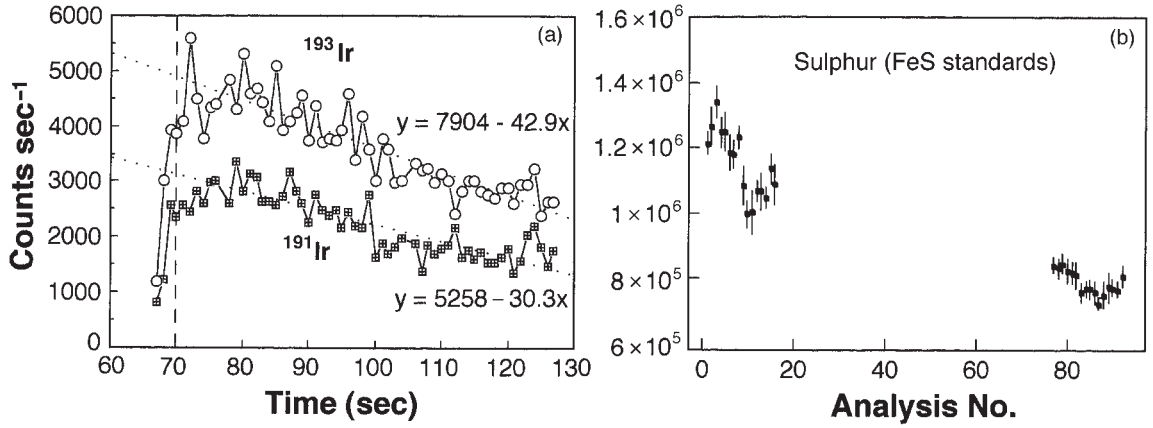

Fig. 4. Correction procedures applied to laser analyses. (a) Correction for time-dependent decreases in count rate during an analysis (our Ir standard). (b) Correction applied for decreases in sensitivity of the quadrupole mass spectrometer with time (S counts rates on our FeS standards over ~4 h). [For details, see Sylvester & Ghaderi (1997).]

Table 3: Average noble metal concentrations in pyrrhotite, in ppm (1σ)

Sample:	B20-17	B20-18	B20-2	B20-4
n:	5	10	6	11
Setting:	normal	normal	pothole	pothole
Os	6·6 (0·9)	9·7 (1·8)	8·5 (1)	10·1 (2·9)
Ir	7 (2·3)	9 (1·1)	6·8 (1)	11·5 (3·9)
Ru	33 (7·5)	31 (7·2)	24 (5·8)	38 (7·4)
Rh	2·2 (0·8)	n.d.	3 (1·4)	4·8 (4·6)
Pt	n.d.	n.d.	1·2 (0·3)	2·7 (2·9)
Pd	n.d.	n.d.	1·5 (1)	n.d.

n.d., not detected.

Table 4: Average noble metal concentrations in pentlandite, in ppm (1σ)

Sample:	B20-17	B20-18	B20-2	B20-4	B20-5
n:	6	10	3	5	10
Setting:	normal	normal	pothole	pothole	normal
Os	7·2 (4·5)	7·6 (4·3)	7 (1·7)	7·8 (4·3)	4·6 (1)
Ir	7·2 (3·4)	8·4 (3·9)	6 (1)	8·2 (3·4)	4·2 (1)
Ru	26 (13)	27 (12)	30 (4·6)	27 (13)	10 (3·3)
Rh	27 (18)	40 (10)	67 (88)	40 (10)	29 (9)
Pt	11 (3·5)	7 (0·7)	9·3 (1·4)	7·2 (0·8)	1·5 (0·3)
Pd	153 (34)	240 (20)	757 (89)	233 (18)	144 (19)

- Os and Ir concentrations in pyrrhotite and pentlandite typically average between 5 and 10 ppm. In both pyrrhotite and pentlandite there is a sharp 1:1 correlation between Os and Ir (Figs 6 and 7), suggesting that both elements substitute into pyrrhotite and pentlandite according to the same crystal chemical rules. In most samples pyrrhotite is slightly enriched in Os and Ir relative to coexisting pentlandite, with a $K_{D\ Os\text{–}Ir}^{po\text{–}pent}$ around 1·2.
- Ru shows a crystal chemical behaviour that is broadly similar to that of Os and Ir. Again, Ru is slightly elevated in pyrrhotite relative to coexisting pentlandite. Although there is a broad relationship between Ru content and total Os + Ir in pyrrhotite and pentlandite (Figs 6 and 7), the correlation is by no means as stringent as it is between Os and Ir.
- Rh and Pd strongly prefer pentlandite over pyrrhotite, Rh by a factor of 10 and Pd by a factor of at least 100. Both elements behave similarly in that neither Rh nor Pd correlate in any systematic way with Os, Ir or Ru (Figs 6 and 7). However, they also do not correlate well with each other—the co-variation of the averages in Table 4 is only apparent and biased by one anomalously high Rh analysis in B20-2.
- Pt is detected in solid solution only in pentlandite although variations between individual spots even on single grains are large and erratic. In pyrrhotite, Pt is commonly below detection limit, with the exception of pyrrhotite in the harzburgitic pothole reef samples B20-2 and B20-4. No correlation exists between Pt and any other PGE (Figs 6 and 7).
- The remaining noble metals (Au and Re) have not been seen in solid solution in any sulphide. Au and Re, together with Pt and some Pd, typically occur as discrete micro-inclusions, and are discussed in a section below.

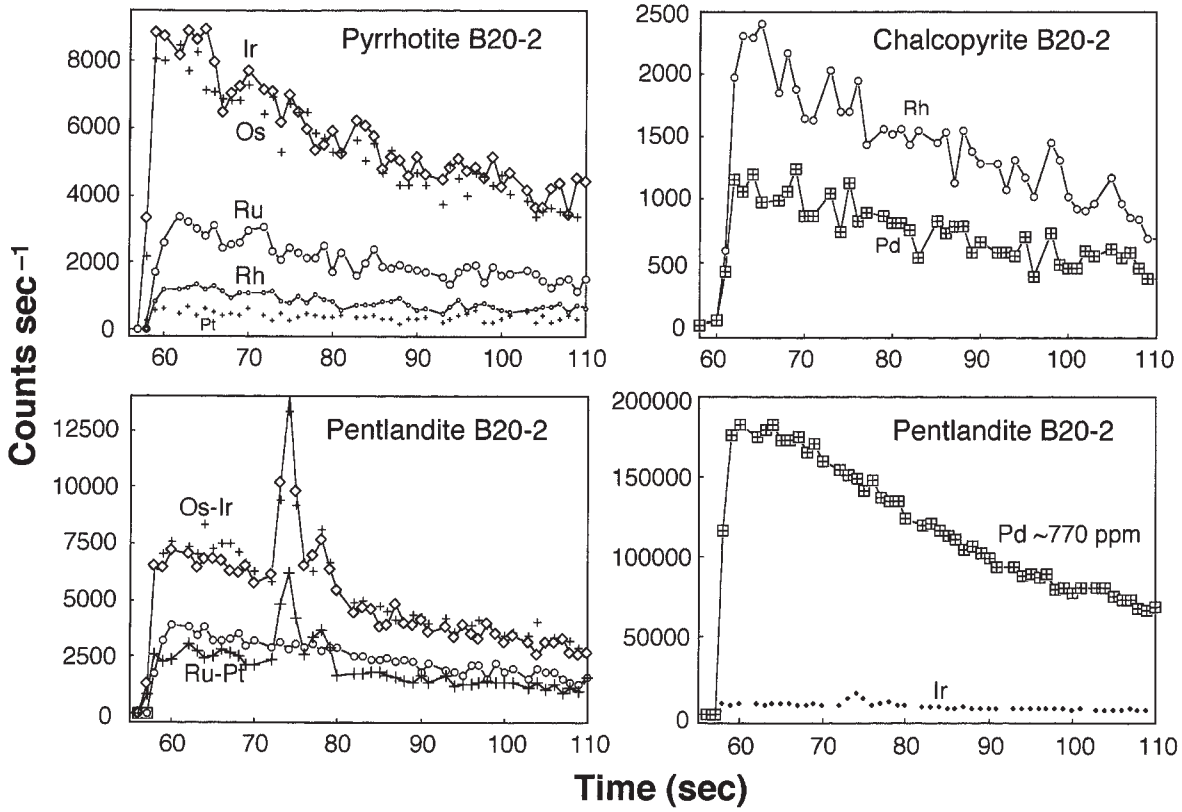

Fig. 5. Typical laser ICP-MS spectra for the three most common types of sulphides in the Merensky Reef—pyrrhotite, pentlandite and chalcopyrite. The two pentlandite spectra are from one analysis, illustrated in separate graphs for reasons of scale. Rh and Pd in chalcopyrite due to interference of $^{40}Ar^{63}Cu$ and $^{90}Ar^{65}Cu$.

We suggest that the above trends were established when magmatic monosulphides recrystallized to pyrrhotite and pentlandite during cooling. Os, Ir and Ru apparently followed Fe and remained soluble in pyrrhotite and pentlandite to the same extent as in the precursor mss. Rh and Pd, on the other hand, fractionated with Ni and now reside in pentlandite. It is probable that the covariations between Os, Ir and Ru in Figs 6 and 7 reflect relict magmatic mss–melt fractionation trends inherited from high-temperature mss, implying that pyrrhotite and pentlandite are undersaturated with respect to Os, Ir and Ru.

A mass balance

In Fig. 8 we normalize the PGE averages in pyrrhotite and pentlandite to CI chondrite abundances (Anders & Grevesse, 1989) and compare these with the CI-normalized bulk sulphide concentrations in Table 1. The purpose is to quantify the proportion of each noble metal in solid solution relative to the proportion in discrete phases. The rationale is as follows: a noble metal whose concentration in solid solution is significantly below its reported bulk sulphide concentration must form discrete phases; a noble metal whose concentration in solid solution is as high as or higher than its average concentration in the bulk sulphide will tend to reside in solid solution. We restrict the mass balance to pyrrhotite and pentlandite as chalcopyrite is so low in PGEs. It should be noted that our approach is only semi-quantitative because exact proportions of pyrrhotite and pentlandite are variable in the Merensky Reef.

The results of the mass balance are as follows (Fig. 8):

- Os and Ir are accommodated easily in solid solution. There is no need for Os and Ir to form discrete phases in the presence of pyrrhotite or pentlandite. To our knowledge, no discrete (micron-sized) Os–Ir-rich PGE phases have been reported from the Merensky Reef.
- Ru abundance in solid solution is slightly lower than Ru concentration in the sulphide concentrate; however, whether this justifies the presence of discrete Ru phases seems doubtful. It appears somewhat surprising that RuS_2 (laurite) is not as rare in the Merensky Reef (see Vermaak & Hendriks, 1976; Kinloch, 1982) as it would appear from Fig. 8. It should be noted, however, that highest Ru concentrations are generally associated

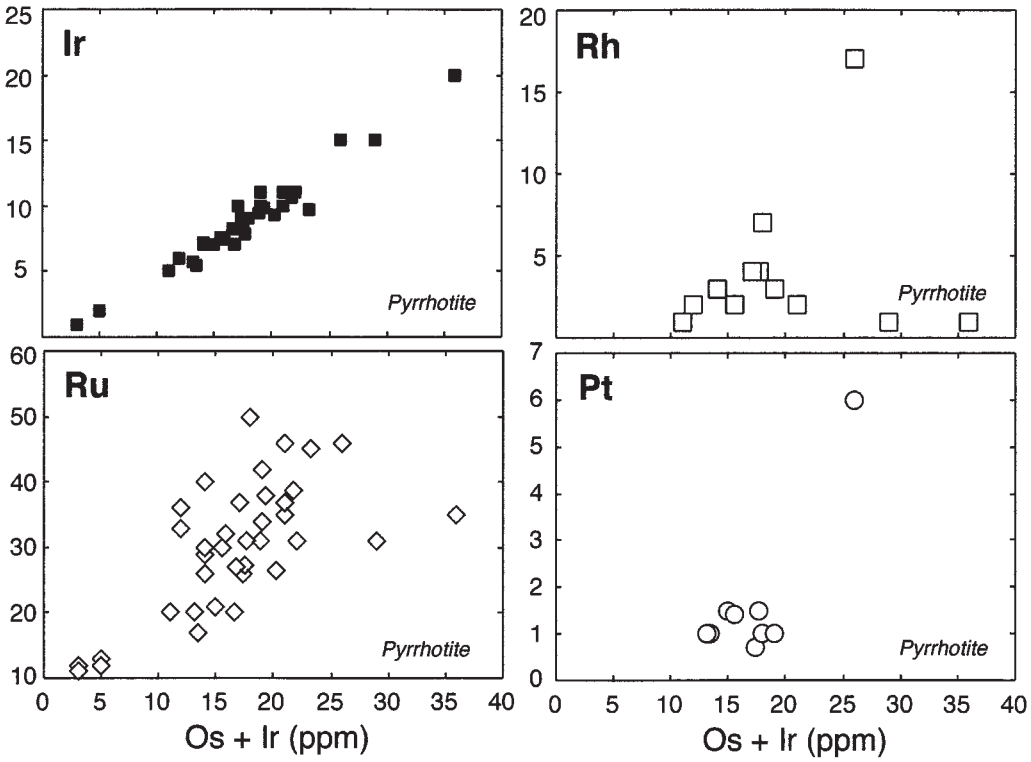

Fig. 6. PGE contents in individual pyrrhotite grains, in ppm.

with the chromite seams (see Fig. 1a) as well as with the UG-2 chromitite, an affinity that is poorly understood anyway.

- Rh is also easily accommodated in solid solution. The Rh deficit in pyrrhotite, relative to bulk ore (Fig. 8), is very nearly compensated for by elevated Rh in pentlandite. Again, Rh-rich PGE phases are rare in the Merensky ore (Vermaak & Hendriks, 1976). It would seem that the presence of discrete Rh phases in the Merensky Reef would require unusually low Ni contents (low pentlandite) in the sulphide ore.
- The presence or absence of discrete Pd-rich phases in magmatic sulphides also critically depends on the Ni content of the ore, as pentlandite is the only phase to take up appreciable Pd. In the Merensky Reef it seems that pentlandite is, on average, not quite abundant enough to accommodate all Pd. Consequently, some proportion of the Pd must reside in discrete mineral phases, and these are mostly inter-metallic compounds with Pt, Bi and Te, as the S_2 fugacity in the Reef for PdS was too low (Barin, 1995).
- Pt is the only noble metal to form discrete phases under nearly all conditions. At low temperature, Pt solubility in Merensky sulphides is far too low to accommodate more than a few percent of the total bulk ore Pt in solid solution.

Thus, our mass balance figures suggest that the only noble metals to reside in discrete noble mineral phases are Pt, Au and some Pd. All others are more or less comfortably held in solid solution, especially in oxidized (S-rich) Merensky sulphide ore (see Ballhaus & Ulmer, 1995). Naturally, our mass balance calculation must be rather simplified, as PGE partitioning in the Merensky sulphide melt must have been influenced by minor elements with chemical affinities to PGEs, notably by As, Bi, Te, Sb and Sn, all common ligands to noble mineral phases. Nevertheless, the general picture agrees reasonably well with the noble metal phase distribution in the Merensky Reef presented by Vermaak & Hendriks (1976).

NOBLE METAL MICRO-INCLUSIONS

An interesting observation is that most sulphides and silicates analysed contain discrete PGE micro-inclusions (see pentlandite in Fig. 5). As laser ablation provides 3-D information on element distribution, in addition to low detection limits to tens of ppb, it has the potential to distinguish between noble metals in solid solution and noble metals that occur as micro-inclusions. One may also approximate inclusion sizes: ablation rates are given

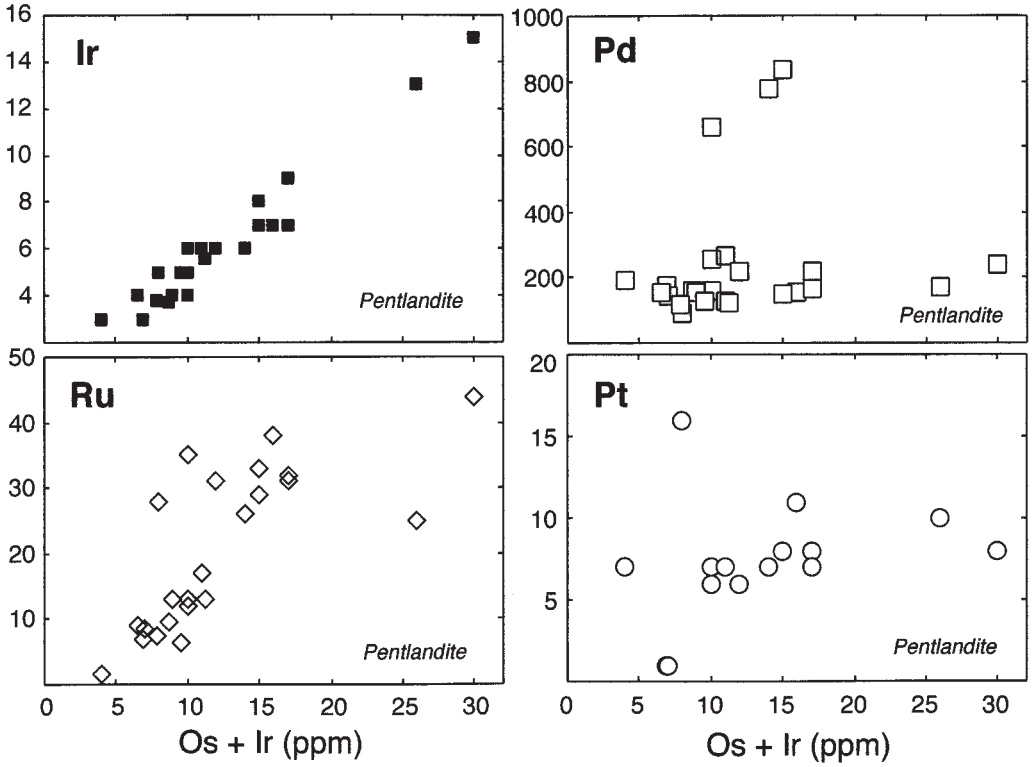

Fig. 7. PGE contents in individual pentlandite grains, in ppm.

by measuring the average depths of ablation pits (1·25 μm/s); as the beam diameter is known (~70 μm) we can readily calculate the volume of material ablated per second (~275 μm^3); we assume that the entire inclusion is consumed in less than 1 s (inclusion diameter less than the ablation rate of 1·25 μm/s); we then recalculate the inclusion peak recorded in terms of ppm PGEs and relate that concentration to the total volume ablated per second (= 100%). This procedure, although rather rough, gives the approximate size of an inclusion in μm^3. We find that maximum inclusion diameters are <100 nm assuming they are spherical in shape.

Inclusions in sulphides

Typical inclusion spectra in sulphides are shown in Figs 9 and 10. The most common types of inclusions have the major element combination Os–Ir–Pt (Fig. 9). They are most abundant in pyrrhotite and pentlandite but have also been encountered in one chalcopyrite and several pyrite–chalcopyrite intergrowths, i.e. phases that do not usually contain Os, Ir or Pt in solid solution. Some inclusions of this kind are polymetallic where Os–Ir–Pt are joined by Ru, Rh and rarely Re. Pd, on the other hand, never participates in inclusion chemistries, neither in pyrrhotite nor pentlandite.

Another common inclusion population is dominated by Pt with variable Pd and sometimes Au (Fig. 10), and in one case Rh. This population appears to be confined to chalcopyrite and chalcopyrite–pyrite intergrowths. Yet another common population has the element combination Pt–Bi–Te, again mostly in chalcopyrite, but exact element ratios cannot be quantified as we did not have standards for Bi and Te. Occasionally, we have also observed near-pure Re and Au inclusions, apparently without any other noble metals.

The exact composition of an inclusions can only be inferred where the element spectrum of an inclusion resembles that of a discrete (microscopically identifiable) noble mineral equivalent. For example, any PGE inclusion with Bi and Te in addition to Pt is almost certainly a submicroscopic equivalent of a bismuthotelluride, one of the most frequent intermetallic phases in the Merensky ore (Vermaak & Hendriks, 1976). Pt ± Pd–Au microinclusions in chalcopyrite presumably are alloys; they are unlikely to be sulphides, as sulphides would not be as flexible in terms of metal combination as alloys, and would reject Au. The most enigmatic compositions certainly are the Os–Ir–Pt inclusions, for no discrete mineral equivalents with that PGE combination have been reported from the Merensky Reef. We infer from their variable PGE ratios that they are also microalloys (see

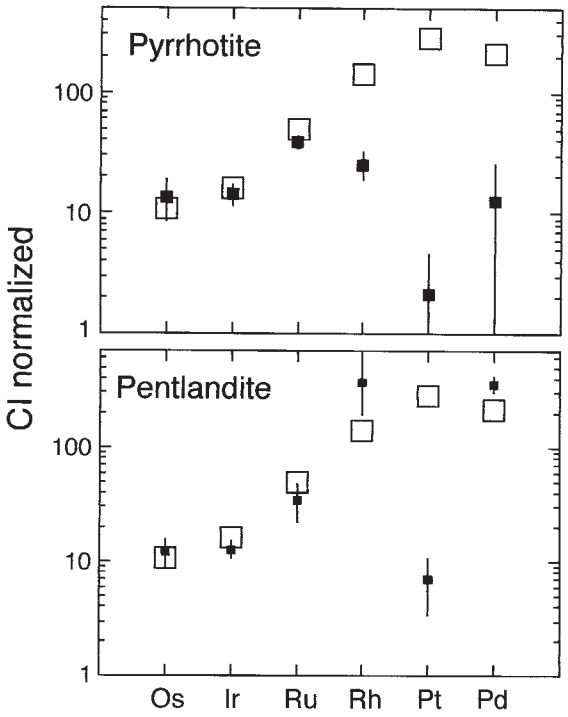

Fig. 8. Mass balance calculations. □, bulk sulphide PGE abundances in Table 1; ■, weighed averages of PGE abundances in pyrrhotite and pentlandite (Tables 3 and 4).

Daltry & Wilson, 1997). Judging from free energy data (Barin, 1995) the S_2 fugacities required to stabilize sulphides with that noble metal composition would be too high to be compatible with the S_2 fugacities of the early Merensky Reef (Ballhaus & Ryan, 1995).

Origins of inclusions

The most interesting aspect of the present study is the origin of the inclusions. Principally, we have two alternatives: (1) subsolidus exsolution from the host sulphides or their high-temperature precursor monosulphides; (2) direct crystallization from the sulphide melt. The second alternative would be most intriguing, for it would imply that the conjugate sulphide–silicate melt system of the Merensky Reef was PGE oversaturated at magmatic temperature.

The Pt–Au and Pt–Bi–Te inclusions in chalcopyrite could be nuclei that crystallized directly from Cu-rich derivative sulphide melts. Fleet *et al.* (1993) have shown experimentally that Pt and Au are incompatible with early monosulphide and tend to concentrate in residual Cu-rich sulphide melts. The same may apply to Bi and Te. As Pt, Au, Bi and Te are not usually metals in solid solution in chalcopyrite, a subsolidus exsolution origin seems rather unlikely.

For the Os–Ir–Pt inclusions we can find arguments both in favour of and against an exsolution origin. If we plot all Os–Ir–Pt inclusions in terms of their three major elements (Fig. 11), ignoring minor Ru and Rh, then it seems indeed that the Os/Ir element ratios in inclusions roughly portray the Os/Ir ratios of the host sulphides, supporting an exsolution origin. On the other hand, there is little reason for pyrrhotite and pentlandite to exsolve Os and Ir if we believe our mass balance arguments (Fig. 8). Also, with respect to other PGEs they show little sensible correlation with the solid solution spectrum of the host sulphide. For example, Os–Ir–Pt inclusions in pyrrhotite never contain any Pd although in ordered low-temperature pyrrhotite Pd is as insoluble as Pt (Ballhaus & Ulmer, 1995). Ru and Rh, if present in inclusions, also do not relate in any systematic way to the PGE solid solution spectrum of the host sulphide.

The fact that Os–Ir–Pt inclusions also occur in chalcopyrite is a good argument against subsolidus exsolution, as chalcopyrite does not carry these elements in solution. Perhaps there are both magmatic and subsolidus features preserved in this inclusion population; for example, it may be that originally magmatic Pt-rich nuggets—Pt being the most common noble metal in the ore and one of the least soluble in silicate melt—became trapped in early monosulphides and then acquired some of the PGEs originally in solid solution as the host sulphide equilibrated during cooling.

Inclusions in silicates and chromite

The best direct proof for a magmatic origin is to find PGE inclusions in high-temperature cumulus silicates. Most suitable for this purpose are olivine and chromite from harzburgitic Reef, because those minerals were the first phases to have crystallized on the liquidus of a primitive silicate Merensky melt, before or contemporaneous with sulphide saturation. Therefore, we have probed cumulus olivine and chromite in sample B20-2 from the harzburgitic pothole Reef (Fig. 1b) whose sulphides proved to be most enriched in PGEs (cf. 770 ppm Pd in pentlandite in Fig. 5).

Typical silicate and chromite spectra are shown in Fig. 12. Nearly half the grains probed contained PGE inclusions, and one olivine was found virtually 'littered' with inclusions. Neither olivine nor chromite contain detectable PGEs in solid solution, contrary to assertions that olivine and chromite can fractionate PGEs (Brügmann *et al.*, 1987; Capobianco *et al.*, 1994). The most common inclusion element is Pt followed by Au and minor anomalies in Pd. Os and Ir, the major PGEs in the pyrrhotite–pentlandite inclusions, are mere traces here and sometimes even offset relative to Pt, as the spectrum of the inclusion-rich olivine in Fig. 12 suggests.

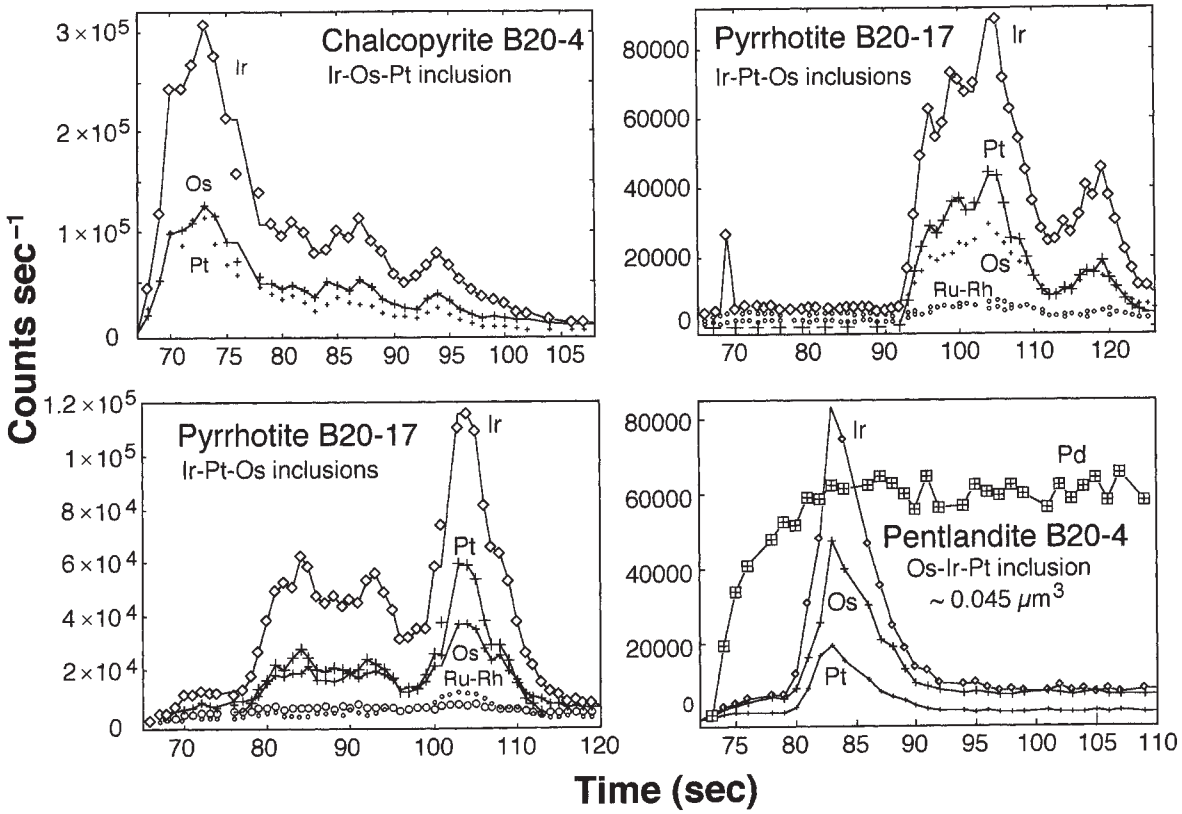

Fig. 9. Laser spectra of Os–Ir–Pt inclusions in sulphides, frequently with minor Ru and Rh. The only noble metals never partitipating in these inclusions are Pd and Au.

Counts for $^{18}O^{16}O$ are not usually elevated by the addition of ^{34}S counts when Pt-rich inclusions are intersected during ablation (compare the chromite spectrum in Fig. 12), so we can probably rule out that we are dealing with late-stage PGE-enriched sulphide melts invading the olivine and chromite along cracks.

DISCUSSION

Clearly, most intriguing are the PGE micro-inclusions. Even if we cannot rule out an exsolution origin, or at least exsolution modification, for some PGE nuggets in sulphides, those in olivine and chromite leave little alternative to PGE saturation at an early cumulus stage, as neither olivine nor chromite carry detectable PGEs in solid solution. Inclusions in olivine are probably PGE nuggets that crystallized from the silicate melt at the same time as olivine and chromite grew. This section will concentrate on the implications of early magmatic PGE saturation for PGE mineralization in the Merensky Reef.

PGE behaviour in silicate and sulphide melts

The solubility of PGEs in silicate melts is very sensitive to oxygen fugacity (Borisov & Palme, 1995, 1997; O'Neill *et al.*, 1995). Generally, the heavy PGEs (Os, Ir and Pt) and Au are found to be less soluble at a given temperature and f_{O_2} than the lighter PGEs. In a melt oversaturated with PGEs, the least soluble noble metals will form nuggets with PGEs and other siderophile elements (Borisov & Palme, 1997).

When a PGE-oversaturated silicate melt exsolves an immiscible sulphide melt, the capacity of the now conjugate silicate–sulphide system to dissolve PGEs will rise dramatically, owing to the large sulphide–silicate PGE partition coefficients. If PGE oversaturation persists after sulphide melt exsolution, a scenario that is likely only if the *R*-factor is very large, one can predict that any existing PGE nugget will immediately fractionate into the sulphide melt. This prediction assumes that the surface energy of a PGE nugget would be lower against a sulphide melt than a silicate melt. Thus, a PGE-oversaturated silicate melt—in chemical exchange equilibrium with the conjugate sulphide melt—will simply

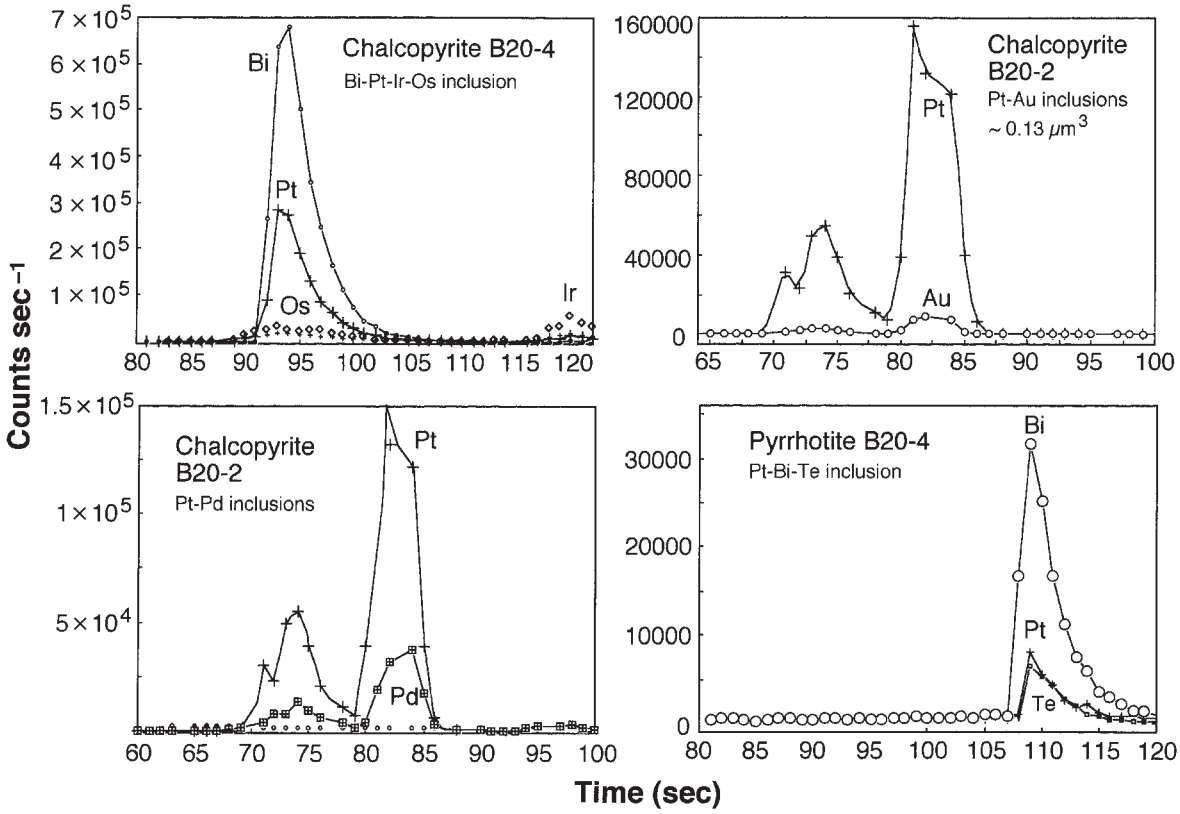

Fig. 10. Pt-rich inclusions (with variable Pd, Au, Bi and Te), most common in chalcopyrite, rare in pyrrhotite and pentlandite.

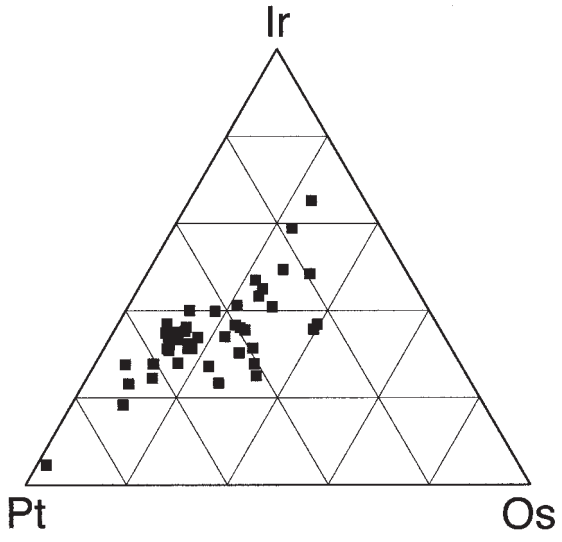

Fig. 11. All Os–Ir–Pt inclusions plotted in terms of their major elements (other PGEs ignored). The principal compositional variable is the concentration of Pt at constant Os/Ir. Os/Ir approximately the same as in the host sulphides for inclusions in pentlandite and pyrrhotite. Some inclusions with minor Ru and Rh. The only noble metals never partitipating in these inclusions are Pd and Au.

transfer all its metal nuclei to the sulphide liquid, without violating partitioning rules. The bulk distribution of the PGEs between silicate and sulphide melt will, however, reflect differences in surface energies of the nuclei in the conjugate melts, rather than actual partition coefficients.

A similar liquid fractionation process was recently described by Ballhaus (1998), albeit in a different system. Ballhaus oversaturated conjugate siliceous and fayalitic melts in the immiscible SiO_2–Al_2O_3–FeO–K_2O system with Cr_2O_3, to simulate nodular ore textures in podiform chromite ores. It was found that chromite nucleated in the immiscible fayalitic melt fraction only while the conjugate siliceous melt remained free of chromite grains; this happened although both melts were chromite oversaturated. The likely explanation is that chromite nucleated preferentially in the fayalitic melt because here crystal–melt interfacial energies were lower. The same is likely to occur in conjugate sulphide–silicate systems oversaturated with respect to the PGEs: a metallic PGE nugget, initially present in the silicate melt, would presumably fractionate into the immiscible sulphide melt once sulphide melt exsolution has occurred.

There is even experimental evidence to this effect. In Fig. 13 we show calculated partition coefficients for Ru, Pd and Pt from the two most recent sets of experimental

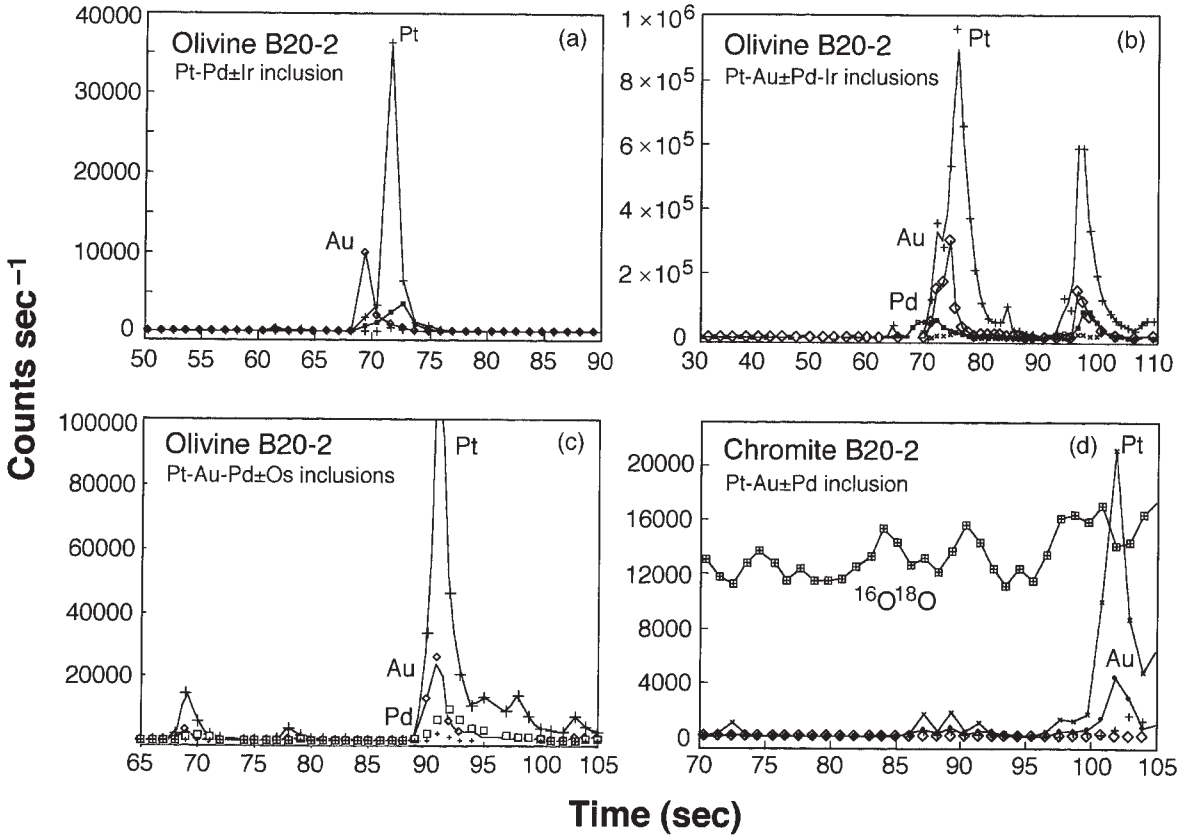

Fig. 12. Pt-rich nuggets in cumulus olivine and disseminated chromite of sample B20-2. Second most abundant noble metal is Au followed by Pd. Minor Os is sometimes slightly offset relative to Pt and Au (separate inclusions?).

studies (Fleet *et al.*, 1996; Crocket *et al.*, 1997), the same *D* values as used in Fig. 3. We have selected only experiments that we consider similar in terms of bulk sulphide Fe/Ni and run temperature. There is a correlation between the PGE content in the sulphide fraction and the calculated partition coefficient, most striking for Ru and Pd. Although there may be several reasons for this correlation (Fleet *et al.*, 1996) it is exactly what one would expect in oversaturated conjugate sulphide–silicate melt systems: the PGE nuclei choose the sulphide melt as preferred nucleation site, and in doing so, they impose a spurious correlation between the apparent partition coefficient and total PGE content of the bulk charge.

Early PGE saturation in the Merensky Reef?

If there was early PGE oversaturation in the Reef then presumably it was with respect to Pt, the most abundant (Table 1) and one of the least soluble metals in the sulphide concentrate. Although the element systematics among the types of PGE inclusions are complex and only partly understood, the sulphur-free Pt-rich nuggets in early cumulus olivine and chromite leave little alternative to early-magmatic PGE saturation. Here we evaluate whether PGE solubility experiments support the notion of early PGE saturation. We test if a silicate melt in equilibrium with a sulphide melt containing the PGE spectrum in Table 1 may be PGE oversaturated at liquidus temperature. We concentrate on Pt, the most abundant and one of the least soluble noble metal of the Merensky ore.

We adopt a sulphide–silicate partition coefficient for Pt of ~6000, i.e. a value at the lower end of the trend in Fig. 13. This yields 47 ppb Pt in the coexisting silicate melt. With regard to oxygen fugacity (f_{O_2}) we tentatively assume that the melt in equilibrium with the Merensky sulphide was close to the equilibrium $C + 2H_2O = CH_4 + CO_2$ (~FMQ – 2 at 0·3 GPa) as graphite is a trace constituent in many Reef sections (Ballhaus, 1988). At FMQ – 2 and 1400°C (i.e. $\log f_{O_2} \sim -6{\cdot}3$), the solubility of Pt in diopside–anorthite eutectic melt is <10 ppb if we extrapolate Borisov & Palme's (1997) highly precise solubility data to that f_{O_2}. This is less than a quarter of the Pt concentration just calculated (i.e. 47 ppb). On this basis it would appear that a silicate melt

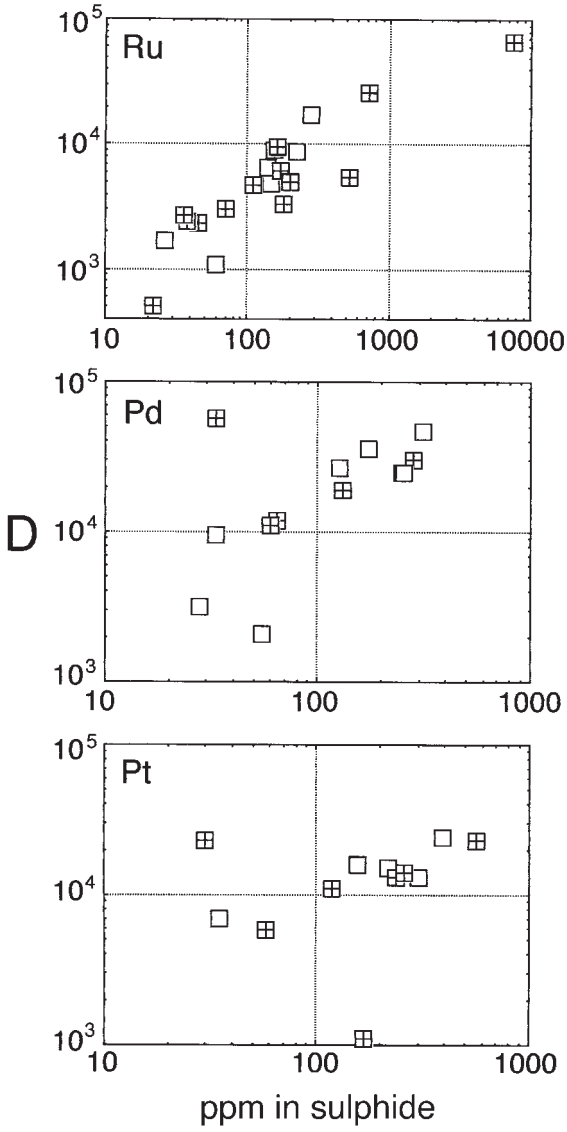

Fig. 13. Compositional dependence of the apparent sulphide–silicate partition coefficients of Ru, Pd and Pt on PGE concentration of the sulphide melt. □, Crocket *et al.* (1997); crossed squares; from Fleet *et al.* (1996).

coexisting with Merensky sulphide melt is Pt oversaturated.

The question is whether or not the experimental diopside–anorthite system is comparable with a natural silicate melt:

- the diopside–anorthite system lacks FeO and S^{2-}, both important components in a silicate melt in equilibrium with sulphide liquid;
- the temperature at which Borisov & Palme (1997) studied Pt solubility is ~200°C higher than the liquidus temperature of most basaltic melts;
- there is uncertainty as to how accurately we can estimate the f_{O_2} of a melt parental to a cumulate horizon such as the Merensky Reef.

With regard to FeO, Borisov (1998) argued that FeO will actually lower Pt solubility relative to the diopside–anorthite eutectic, by a factor of at least two. He noted that Fe combines with Pt and promotes (Pt,Fe) nugget formation. We can probably extend this to the other PGEs, as well to Bi and Te; all these elements are present in the sulphide concentrate, all compete with Pt for the same structural sites in the silicate melt, and all are known to be ligands to Pt in natural mineral phases; hence, they are also likely to suppress Pt solubility.

With regard to sulphur, dissolved S^{2-} may enhance Pt solubility relative to Borisov & Palme's (1997) eutectic melt. However, the actual effect may be very small considering how little S^{2-} there is in a silicate melt relative to O^{2-} (O'Neill *et al.*, 1995) even in an S-saturated melt.

With regard to temperature, we assume that lowering temperature from 1400°C (the experimental system) to 1200°C (a liquidus temperature for the early Merensky Reef) will lower Pt solubility considerably. It should be noted, however, that the temperature effect on Pt solubility recorded by Borisov & Palme (1997) was not clear-cut, although we think this is an experimental problem.

The largest uncertainty comes from trying to estimate magmatic f_{O_2}, as a change of one log unit in f_{O_2} shifts the solubility of Pt in a silicate melt by an order of magnitude (Borisov & Palme, 1997). It is difficult to deduce a magmatic oxidation state from phase compositions and parageneses in a slowly cooled cumulate horizon. Perhaps we cannot use graphite as a magmatic f_{O_2} indicator, as graphite is not proven to be a magmatic phase in the Merensky Reef. On the other hand, an f_{O_2} around FMQ – 2 is reasonable for a tholeiitic melt that intruded carbonaceous metasediments of the Archaean Transvaal system and precipitated graphite at some stage, even if it was not at the early cumulus stage (see Ballhaus, 1988).

In summary, weighing the above arguments, it does not seem unrealistic to conclude that the silicate melt that coexisted with the PGE-enriched Merensky sulphide melt (i.e. Table 1) was oversaturated with respect to the least soluble PGEs, notably with Pt.

A model for PGE concentration in the Merensky Reef

If the silicate melt was oversaturated with respect to some PGEs, an exsolving sulphide liquid merely serves as a collector to preserve a pre-existing stratiform PGE anomaly in the liquid-stratified magma chamber. A possible model is illustrated in Fig. 14.

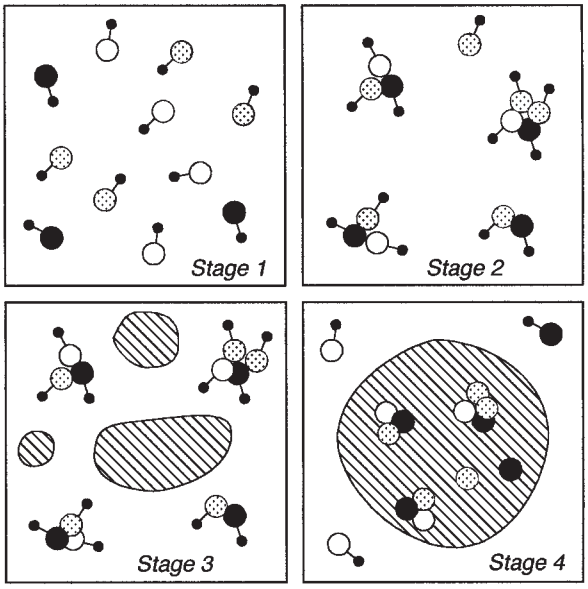

Fig. 14. A model for PGE enrichment processes in conjugate sulphide–silicate melt systems oversaturated with respect to PGEs (see text). It is assumed that the noble metals, here represented by differently shaded symbols, are dissolved in the sulphur-saturated silicate melt principally as binary metal–oxide and metal–sulphide complexes before they cluster to form nuggets; nuggets in the sulphide phase are assumed to be metallic.

- Stage 1 illustrates an early primitive pre-Merensky silicate melt undersaturated with respect to PGEs; the individual PGEs, represented by differently shaded symbols, are dissolved in the melt structure as simple binary PGE–O and/or PGE–S complexes.
- In stage 2 the melt has become oversaturated with respect to some PGEs following continued enrichment; in response, complex formation sets in, as predicted by Tredoux *et al.* (1995), i.e. the least soluble metals combine to polymetallic complexes with other PGEs and possibly other metals (e.g. Bi, Te, Fe, etc.) with siderophile affinities, in an effort to minimize their chemical potentials. Silicates and chromite crystallizing at this stage trapped some PGE nuggets.
- In stage 3 S saturation has occurred, possibly as a result of a replenishment episode, or contamination of primitive liquid by more evolved siliceous melt, or FeO depletion by chromite precipitation, and/or any other process that triggers S saturation; droplets of monosulphide liquid exsolve.
- Stage 4 illustrates capture of PGE nuggets by the exsolving sulphide melt; the metallic PGE micro-alloys all fractionate into the sulphide liquid, where interfacial energies are lower. The PGE spectrum of the PGE anomaly in the stratified magma chamber is preserved unchanged, as PGE sulphide–silicate partition coefficients do not play a significant role during this capturing process. The sulphide melt merely immobilizes a pre-existing *in situ* stratiform PGE anomaly in the silicate melt, unfractionated with respect to the parent silicate melt PGE ratios.

The problem of PGE enrichment

The model presented in Fig. 14 provides no answer as to how the PGEs became enriched in the first place. In principle, it is possible that PGE nuggets were collected from the magma column above the Reef, in much the same fashion as in the model of Campbell *et al.* (1983; see Cawthorn, 1998). The only modification to the *R*-factor model would be that PGE partitioning into exsolved dispersed sulphide would be controlled by surface energies of early-magmatic PGE nuclei against sulphide melt rather than actual partition coefficients based on PGE solubilities in the conjugate melts.

However, field evidence argues against PGE collection 'from above'. Figure 1b–d illustrates local deviations in Merensky Reef facies around and within pothole disturbances. There are many underground exposures where sulphide-bearing mineralized Merensky Reef, both as contact reef and as thick pegmatoidal reef, occurs along overturned pothole flanks. Moreover, within potholes, Reef can be seen undercutting horizons of its footwall sequence for several metres (Ballhaus, 1988) and still remain sulphide–PGE mineralized. Clearly, these are examples that are hard to envision with any type of large-scale crystal mush settling from 'above' onto the magma chamber floor, which is the backbone of the *R*-factor model. It should be noted that we do not deny the role of magma addition at Merensky times (Kruger & Marsh, 1982); however, the magma added flowed directly onto the chamber floor and had little chance to equilibrate globally with the overlying resident melt (Ballhaus & Ryan, 1995).

The alternative to enrichment from 'above' is that the PGEs became enriched from 'below' by bottom growth processes (McBirney & Noyes, 1979; Morse, 1986), i.e. accumulated ahead of an advancing crystallization front in a chemically stagnant boundary layer, ultimately nucleating nuggets. This model, however, incurs as many problems as mineralization from 'above'. The ore grades of the Merensky Reef are, over a stoping width of 1 m, ~8 ppm total PGEs + Au, in the proportions summarized in Table 1. In Davies & Tredoux's (1985) high-magnesian basalt there is ~37 ppb combined PGE plus Au, in about the same proportions as in the bulk sulphide concentrate. If one assumes that PGE upward concentration was near-perfect, the Reef houses the essentials of >200 m of a primitive basaltic melt column. At Union Section, however, the minimum vertical separation between the Merensky Reef and the next lower PGE-rich horizon in the stratigraphy, the UG-2, is only 35 m (see Viljoen *et al.*, 1986).

A more serious argument against enrichment from 'below' than our simple-minded mass balance is that the unmineralized cumulates below the Reef do not seem to be depleted in total PGEs relative to the parental silicate melts. Maier & Barnes (1998) found that the 'PGE barren' cumulates of the lower and lower critical zones contain, on average, around 30–40 ppb combined noble metals although not necessarily in the pristine proportions observed in basaltic melt. The footwall cumulates are not depleted in noble metals when compared with average basalt. We do not see a depletion in terms of absolute PGE contents in the footwall that would complement the PGE anomalies in the ore horizons.

CONCLUSIONS

The chondrite-normalized noble metal spectrum of the sulphide concentrate of the Merensky Reef is essentially identical to PGE spectra of typical low-pressure basaltic melts. Unless the sulphide–silicate partition coefficients are all the same, it is difficult to envision how the *R*-factor model can explain PGE enrichment in the Merensky Reef. Nevertheless, enrichment must be magmatic even though we may not fully understand the process; it is hard to imagine how large-scale fluid transport could transpose an essentially basaltic PGE spectrum unchanged into the sulphide ore.

The PGE micro-inclusions in olivine and chromite suggest that the magma preceding the Merensky Reef was PGE oversaturated at liquidus temperature before sulphide saturation occurred. As a result, the least soluble PGEs crystallized as metallic nuggets along with other siderophile elements. Some of the early nuggets are preserved as micro-inclusions in early cumulus phases such as olivine and chromite.

It seems that sulphide melt does not play a major role in enriching PGEs to stratiform PGE anomalies in layered intrusions (Tredoux *et al.*, 1995). In the Merensky Reef, its role was to 'immobilize' a pre-existing, stratiform PGE concentration in the liquid-stratified magma chamber that was unfractionated with respect to PGE ratios in primitive basaltic melt. It should be noted, however, that the presence of a sulphide melt is not essential in preserving a stratiform PGE anomaly. There are examples in other layered intrusions of sulphide-free stratiform PGE anomalies that are distinctly offset relative to stratiform sulphide anomalies (Barnes, 1995).

ACKNOWLEDGEMENTS

Chris Ballhaus thanks Dave Ellis (ANU) for making available his high-pressure facilities, and Richard Arculus for his invitation to ANU. Comments on the manuscript by Mark Rehkämper, Jean-Pierre Lorand, M. J. O'Hara, Grant Cawthorn, and an anonymous referee are highly appreciated. This work was supported by the Heisenberg-Referat of DFG (Grant Ba 964/4-1) and by ARC (Grant A39602510 to R. J. Arculus). This is GEMOC Publication 182.

REFERENCES

Anders, E. & Grevesse, N. (1989). Abundances of the elements: meteoritic and solar. *Geochimica et Cosmochimica Acta* **53**, 197–214.

Ballhaus, C. (1988). Potholes of the Merensky Reef at Brakspruit shaft, R.P.M.—primary disturbances in the magmatic stratigraphy. *Economic Geology* **83**, 1140–1158.

Ballhaus, C. (1998). Origin of podiform chromite deposits by magma mingling. *Earth and Planetary Science Letters* **156**, 185–193.

Ballhaus, C. & Ryan, C. G. (1995). Platinum-group elements in the Merensky Reef. I. PGE in solid solution in base metal sulphides and the down-temperature equilibration history of Merensky ores. *Contributions to Mineralogy and Petrology* **122**, 241–251.

Ballhaus, C. & Ulmer, P. (1995). Platinum-group elements in the Merensky Reef: II. Experimental solubilities of platinum and palladium in $Fe_{1-x}S$ from 950 to 450°C under controlled f_{S2} and f_{H2}. *Geochimica et Cosmochimica Acta* **59**, 4881–4888.

Ballhaus, C. & Stumpfl, E. F. (1986). Suphide and platinum mineralization in the Merensky Reef: evidence from fluid inclusions. *Contributions to Mineralogy and Petrology* **94**, 193–204.

Barin, I. (1995). *Thermochemical Data of Pure Substances*. Weinheim: VCH Verlagsgesellschaft.

Barnes, S. J. (1995). Partitioning of the platinum-group elements and gold between silicate and sulphide magmas in the Munni Munni Complex, Western Australia. *Geochimica et Cosmochimica Acta* **57**, 1277–1290.

Barnes, S. J. & Naldrett, A. J. (1985). Geochemistry of the J-M (Howland) Reef of the Stillwater Complex, Minneapolis adit area. I. Sulfide chemistry and sulfide–olivine equilibrium. *Economic Geology* **80**, 709–729.

Bezmen, N. I., Asif, M., Brügmann, G. E., Romanenko, I. M. & Naldrett, A. J. (1994). Distribution of Pd, Ru, Rh, Ir, Os, and Au between sulphide and silicate melts. *Geochimica et Cosmochimica Acta* **58**, 1251–1260.

Borisov, A. (1998). Noble metal solubilities in FeO-containing melts: estimates based on experiments in FeO-free systems. *EOS Supplement, American Geophysical Union, Spring Meeting*, S373.

Borisov, A. & Palme, H. (1995). Solubility of Ir in silicate melts: new data from experiments with $Ir_{10}Pt_{90}$ alloys. *Geochimica et Cosmochimica Acta* **59**, 481–485.

Borisov, A. & Palme, H. (1997). Experimental determination of the solubility of platinum in silicate melts. *Geochimica et Cosmochimica Acta* **61**, 4349–4357.

Boudreau, A. E., Mathez, E. A. & McCallum, I. S. (1986). Halogen geochemistry of the Stillwater and Bushveld Complexes: evidence for transport of the platinum-group elements by Cl-rich fluids. *Journal of Petrology* **27**, 967–986.

Brügmann, G. E., Arndt, N. T., Hofmann, A. W. & Tobschall, H. J. (1987). Noble metal abundances in komatiite suites from Alexo, Ontario, and Gorgona Island, Columbia. *Geochimica et Cosmochimica Acta* **51**, 2159–2169.

Capobianco, C. J., Hervig, R. L. & Drake, M. J. (1994). Experiments on crystal/liquid partitioning of Ru, Rh, and Pd for magnetite and

hematite solid solutions crystallized from silicate melts. *Chemical Geology* **113**, 23–43.

Campbell, I. H. (1987). The distribution of orthocumulate textures in the Jimberlana Intrusion. *Journal of Geology* **95**, 35–54.

Campbell, I. H., Naldrett, A. J. & Barnes, S. J. (1983). A model for the origin of the platinum-rich sulphide horizons in the Bushveld and Stillwater Complexes. *Journal of Petrology* **24**, 133–165.

Cawthorn, R. G. (1998). Controls on platinum mineralisation in the Bushveld Complex. *8th International Platinum Symposium, Geological Society of South Africa Symposium Series* **S18,** 67–69.

Crocket, J. H., Fleet, M. E. & Stone, W. E. (1997). Implications of composition for experimental partitioning of platinum-group elements and gold between sulphide liquid and basalt melt: the significance of nickel content. *Geochimica et Cosmochimica Acta* **61**, 4139–4149.

Daltry, V. D. C. & Wilson, A. H. (1997). Review of platinum-group mineralogy: compositions and elemental associations of the PG-minerals and unidentified PGE-phases. *Mineralogy and Petrology* **60**, 185–229.

Davies, G. & Tredoux, M. (1985). The platinum group element and gold content of the marginal rocks and sills of the Bushveld Complex. *Economic Geology* **80**, 838–848.

Fleet, M. E., Chryssoulis, S. L., Stone, W. E. & Weisener, C. G. (1993). Partitioning of platinum-group elements and Au between sulphide liquid and basalt melt. *Contributions to Mineralogy and Petrology* **115**, 36–44.

Fleet, M. E., Crocket, J. H. & Stone, W. E. (1996). Partitioning of platinum-group elements (Os, Ir, Ru, Pt, Pd) and gold between sulphide liquid and basalt melt. *Geochimica et Cosmochimica Acta* **60**, 2397–2412.

Kinloch, E. D. (1982). Regional trends in the platinum-group mineralogy of the critical zone of the Bushveld Complex, South Africa. *Economic Geology* **77**, 1328–1347.

Kruger, F. J. & Marsh, J. S. (1982). Significance of $^{87}Sr/^{86}Sr$ ratios in the Merensky cyclic unit of the Bushveld Complex. *Nature* **298**, 53–55.

Li, C., Barnes, S.-J., Makovicky, E., Rose-Hansen, J. & Makovicky, M. (1996). Partitioning of nickel, copper, iridium, rhodium, platinum and palladium between monosulfide solid solution and sulphide liquid: effects of composition and temperature. *Geochimica et Cosmochimica Acta* **60**, 1231–1238.

Maier, W. D. & Barnes, S.-J. (1998). Platinum-group elements of the lower, critical, and main zones of the Bushveld Complex. Extended abstract, *8th International Platinum Symposium, Geological Society of South Africa Symposium Series* **S18,** 221–223.

McBirney, A. R. & Noyes, R. M. (1979). Crystallization and layering of the Skaergaard intrusion. *Journal of Petrology* **20**, 487–554.

Morse, S. A. (1986). Convection in aid of adcumulus growth. *Journal of Petrology* **27**, 1183–1214.

Naldrett, A. J., Cameron, G., Von Gruenewaldt, G. & Sharpe, M. R. (1987). The formation of stratiform PGE deposits in layered intrusions. In: Parsons, I. (ed.) *Origins of Igneous Layering*. Dordrecht: D. Reidel, pp. 313–397.

O'Neill, H. St C., Dingwell, D. B., Borisov, A., Spettel, B. & Palme, H. (1995). Experimental petrochemistry of some highly siderophile elements at high temperatures, and some implications for core formation at the mantle's early history. *Chemical Geology* **120**, 255–273.

Perkins, W. T. & Pearce, N. J. G. (1995). Mineral analysis by laserprobe inductively coupled plasma mass spectrometry. In: Potts, P. J., Bowles, J. F. W., Reed, S. J. B. & Cave, M. R. (eds) *Microprobe Techniques in the Earth Sciences. The Mineralogical Society Series 6*. London: Chapman & Hall, pp. 291–325.

Sylvester, P. J. & Eggins, S. M. (1997). Analysis of Re, Au, Pt, Pd and Rh in NIST glass certified reference materials and natural basalt glasses by laser ablation-ICP-MS. *Geostandards Newsletter* **21**, 215–229.

Sylvester, P. J. & Ghaderi, M. (1997). Trace element analysis of scheelite by excimer laser ablation-inductively coupled plasma mass spectrometry (ELA-ICPMS) using a synthetic silicate glass standard. *Chemical Geology* **141**, 49–65.

Tredoux, M., Lindsay, N. M., Davies, G. & McDonald, I. (1995). The fractionation of platinum-group elements in magmatic systems, with the suggestion of a novel causal mechanism. *South African Journal of Geology* **98**, 157–167.

Vermaak, C. F. & Hendriks, L. P. (1976). A review of the mineralogy of the Merensky Reef, with specific reference to new data on the precious metal mineralogy. *Economic Geology* **71**, 1244–1269.

Viljoen, M. J., De Klerk, W. J., Coetzer, P. M., Hatch, N. P., Kinloch, E. & Peyerl, W. (1986). The Union section of Rustenburg Platinum Mines Limited with reference to the Merensky Reef. In: Anhaeusser, C. R. & Maske, S. (eds) *Mineral Deposits of Southern Africa, Vol. 2*. Johannesburg: Geological Society of South Africa, pp. 1061–1090.